Attenuated total reflectance Fourier transform infra-red studies of crystalline–amorphous content on polyethylene surfaces

J. B. Huang, J. W. Hong and M. W. Urban*
Department of Polymers and Coatings, North Dakota State University, Fargo, ND 58102, USA
(Received 12 September 1991; revised 28 January 1992; accepted 26 March 1992)

Intensity ratios of the bands due to CH_2 bending and rocking normal vibrations, used as a measure of the surface crystallinity in polyethylene, are examined by attenuated total reflectance Fourier transform infra-red (ATR *FT*i.r.) spectroscopy. This study shows that the ATR optical dispersions and the orientation of surface crystallites have a substantial effect on the crystallinity measurements. It appears that improper analysis of strong, overlapping i.r. bands in the ATR spectra may generate systematic errors. While the optical effects associated with ATR measurements can be accounted for and corrected by the use of the Kramers–Kronig transform and Fresnel's equation, determination of the crystallinity gradients and orientation of the crystallites requires detailed polarization studies and theoretical considerations.

(Keywords: ATR *FT*i.r. spectroscopy; polyethylene; crystallinity)

INTRODUCTION

Although many papers are published every year dealing with i.r. spectroscopy of polyethylene, only a limited number address the issues related to the structures that develop on polyethylene surfaces. The primary focus of previous studies has been on the spectroscopic determination of crystallinity[1–6] and defect structures[7–12] in polyethylene. Because crystalline content affects many macroscopic properties, its determination is of primary importance. In the initial studies, crystallinity was determined by ratioing the intensities of the band at $1303\,cm^{-1}$ due to the amorphous phase in solid and molten states[13]. Because this approach uses one band in two spectra, it suffers from uncertainties attributed to the differences between absorption coefficients in solid and molten states. Furthermore, uncontrollable changes of the film thickness on melting are one of the major sources of experimental errors. Later on, measurements involving one band in one spectrum were developed for the amorphous band at $1303\,cm^{-1}$, for which a universal calibration constant was established[14]. In this case, crystallinity calculations also require the values of thickness and density of the films. This approach was extended to other bands, including the band at $730\,cm^{-1}$ due to CH_2 rocking vibrations of the crystalline phase[14]. The $730\,cm^{-1}$ band, however, was not preferred due to its sensitivity to the polymer chain orientation[14]. Although in all cases baseline correction and curvefitting procedures are required[15], it is generally accepted that a more convenient and reliable method involves the use of the two bands at $1894\,cm^{-1}$ due to the crystalline phase and the band at $1303\,cm^{-1}$ due to the amorphous phase[16].

While measurements of the bulk polyethylene properties are of significant importance, the surface content appears to be of increasing interest because it may affect such properties as adhesion, durability and other macroscopic functions. For that reason, topological inhomogeneity and distribution of the crystalline and amorphous phases on polyethylene surfaces have been the subject of recent studies[17,18]. Attenuated total reflectance Fourier transform infra-red (ATR *FT*i.r.) spectroscopy was employed in these studies.

Similar to the i.r. transmission spectrum, the ATR spectrum of polyethylene contains two bands due to pure crystalline ($1894\,cm^{-1}$) and pure amorphous ($1303\,cm^{-1}$) normal modes, but unfortunately these bands are too weak to be used for ATR quantitative analysis. Therefore, more intense bands, such as the CH_2 bending (1474 and $1464\,cm^{-1}$) and rocking (730 and $720\,cm^{-1}$) normal vibrations should be employed. The bands at 1474 and $730\,cm^{-1}$ are due to the crystalline phase only, whereas the bands at 1464 and $720\,cm^{-1}$ represent contributions from both the crystalline and amorphous phases. Recently, these bands were used to determine the amorphous content (x), following the empirical relationship given below[17]:

$$x = \frac{I_b - I_a/1.233}{I_a + I_b} \times 100 = \frac{1 - (I_a/I_b)/1.233}{1 + I_a/I_b} \times 100 \quad (1)$$

where I_a and I_b are the intensities of the 730 and $720\,cm^{-1}$ or 1474 and $1464\,cm^{-1}$ bands, respectively, The constant (1.233) in equation (1) represents the intensity ratios of these bands in the spectrum of purely crystalline

* To whom correspondence should be addressed

0032-3861/92/245173-06

polyethylene and was derived using the factor group splitting applied to a single polyethylene crystal[19]. The key spectral features used in this method are the experimentally determined intensity ratios, I_a/I_b, obtained from the spectrum of the semicrystalline sample, and the theoretical values of the ratios for pure crystalline polyethylene. This approach was applied to commercial polyethylene films, from which it was concluded that the crystallinity of polyethylene was considerably higher near the surface. In this study, we address and question two issues that may significantly affect the I_a/I_b intensity ratio used in the analysis of polyethylene surface by ATR *FT*i.r. spectroscopy: (1) distortion of intense i.r. bands in ATR spectra due to the nature of the measurements caused by optical dispersions; and (2) orientation of the crystallites on the polyethylene surface. In an effort to address these issues we will utilize well established optical theories[20] developed specifically for the analysis of strong ATR bands[21].

EXPERIMENTAL

Commercially available polyethylene film (Glad Cling Wrap) was used in the ATR *FT*i.r. depth profiling studies. The direction of unrolling is referred to as the machine direction of the film.

All spectra were measured on a Digilab FTS-20 *FT*i.r. spectrometer. A Spectra-Tech ATR accessory, equipped with a KRS-5 crystal ($3 \times 20 \times 50\,mm^3$, end-face bevelled at 45°) and a 0.4 μm wire grid polarizer (Spectra-Tech Ltd) were used in the surface depth profiling studies. The polarizer was placed between the i.r. source and the ATR attachment in such a way that the electric vector of the polarized light was perpendicular to the plane of incidence defined by the incident and reflected light beams and referred to as s-polarized light. In the orientation studies, the polarization direction of the incident light was fixed, whereas the sample orientation relative to the laboratory axis was varied.

ATR *FT*i.r. spectra were transferred to an IBM compatible computer for further analysis using Spectra Calc™ software*. Because the Beer–Lambert law cannot be directly applied to intense ATR bands, the spectra were first converted to reflectivity for each reflection and then to absorbance per unit length following the procedure described by Bardwell and Dignam[21]. The double Fourier transform approach used in their procedure for the numerical Kramers–Kronig transformation was replaced by the Maclaurin formula. The latter has been shown to have superior accuracy to the double Fourier transform[22]. A comparison of this and other procedures[23] will be shown in a separate publication[24].

The depth of penetration is evaluated according to the following equation[25]:

$$d_p = \frac{\lambda_2}{2\pi(\sin^2\theta - n_{21}^2)^{1/2}} \tag{2}$$

where $n_{21} = n_2/n_1$ (n_2 is the refractive index of the sample and n_1 is the refractive index of the ATR crystal), λ_1 ($=\lambda/n_1$) is the wavelength in the ATR crystal and θ is the angle of incidence. The angle of incidence was corrected according to the manual of the ATR attachment. In this study, the penetration depths at $720\,cm^{-1}$ were calculated using $n_1 = 2.38$ (KRS-5) and $n_2 = 1.5$ (polyethylene). It should be noted that the use of a real, constant value for n_2 may contain an error in the calculations of the penetration depth. This approach was chosen to simplify a comparison with the previous studies. Although the use of a complex refractive index is more appropriate, it should be realized that for strongly absorbing and stratified samples, the amplitude of the evanescent wave does not follow a simple exponential decay[26]. Therefore, the concept of depth of penetration may no longer be relevant.

RESULTS AND DISCUSSION

Although the fundamental principles of ATR spectroscopy are well documented[20], the methodologies for quantitative analysis have often been diversified. Therefore, before the ATR spectra of polyethylene are analysed, let us first establish methodologies used for quantitative analysis of ATR spectra and relate them to the surface crystallinity problem.

One approach is to treat ATR *FT*i.r. spectra as if they were recorded in a transmission mode of detection. In an effort to use the Beer–Lambert law for quantitative analysis, a quantity called effective thickness, d_e, is introduced and defined by the following equation:

$$\mathrm{ATR}(\nu) \equiv \log\left(\frac{I_{in}}{I_{re}}\right) = \beta(\nu) d_e(\nu) \tag{3}$$

where I_{in} and I_{re} are the incident and reflected light intensities and $\beta(\nu)$ is the absorbance per unit length. Because d_e depends on the polarization of the incident light, polarized light should be used to simplify the expression. The effective thicknesses for perpendicular and parallel polarizations, respectively, are given by the following equations[27].

$$d_{e\perp} = \frac{n_{21}\lambda_1 \cos\theta}{\pi(1-n_{21}^2)(\sin^2\theta - n_{21}^2)^{1/2}} \tag{4}$$

and

$$d_{e\parallel} = \frac{n_{21}\lambda_1(2\sin^2\theta - n_{21}^2)\cos\theta}{\pi(1-n_{21}^2)(1+n_{21}^2)(\sin^2\theta - n_{21}^2)^{3/2}} \tag{5}$$

These equations can be derived assuming that the total reflectance $R = 10^{-\beta d_e} \approx 1 - 2.303\beta d_e$ and ignoring non-linear terms in the series expansion of the Fresnel reflectivity. Therefore, n_2 in the above equations represents the real part of the complex refractive index. Because the above equations are only valid for weak bands, it is also reasonable to ignore the dispersion in n_2. As seen from equations (3)–(5), under such conditions, the ATR spectrum multiplied by wavenumber differs from the true absorbance spectrum $\beta(\nu)$ by a scaling factor only. Therefore, conventional techniques for quantitative analysis such as band ratioing, normalization against an internal standard band, and spectral subtractions can be used[28]. As a matter of fact, several successful applications of these data processing techniques were reported[29–31]. It should be realized, however, that for strong bands neither non-linear terms in the Fresnel reflectivity expansion series nor the dispersion of n_2 can be ignored. As a matter of fact, considerable frequency shifts and intensity changes in ATR spectra

* Array Basic is a Basic computer programming language developed for the use in a Spectra Calc environment. Both Array Basic and Spectra Calc are the software products of Galactic Industries Corporation

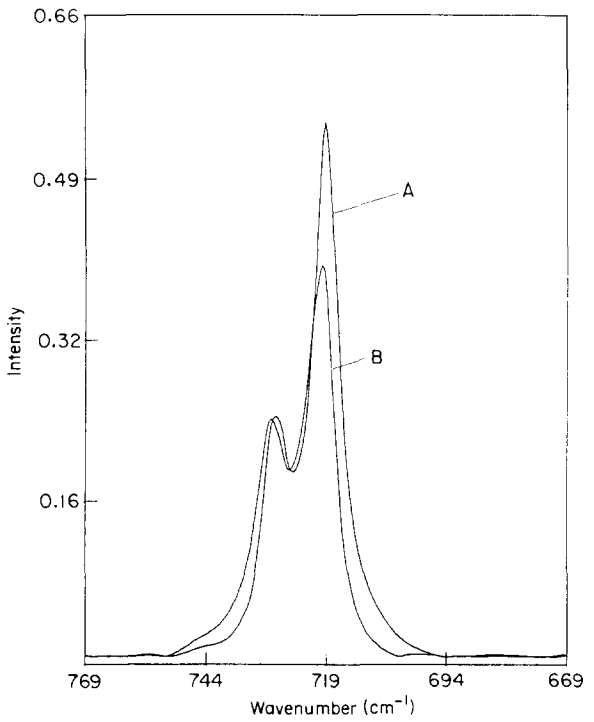

Figure 1 Raw (A) and corrected (B) ATR *FT*i.r. spectra of polyethylene recorded at a 45° angle of incidence with the sample machine direction perpendicular to the electric vector of the s-polarized light

relative to the true absorbance spectrum have been reported for such cases[32,33], further substantiating concerns that previous efforts may require additional considerations.

In an effort to avoid spectral distortions of strong ATR bands, Fresnel's equation[34], employed for the total reflectance of the light at the interface of two homogeneous media of infinite thickness, was used[20]. Following the use of Fresnel's equation and taking into account a given experimental set-up, the factor that primarily affects reflectance is the complex refractive index of the sample. A detailed discussion on the macroscopic and microscopic aspects of the complex refractive index has been presented by Crawford *et al.*[32]. In essence, the real and imaginary parts of the complex refractive indices are related to each other by the Kramers–Kronig transform (KKT). If the refractive index of the sample in a non-absorbing region is known, both parts of the complex refractive indices can be calculated from the measured ATR spectra[21,23,35]. The imaginary part, referred to as the absorption index, can be converted to a new, corrected spectrum expressed as absorbance per unit length of the sample. The latter can also be determined from transmission measurements on thin films[36,37]. The absorbance spectrum can then be further analysed using conventional data-processing techniques. This methodology provides suitable results if the sample is homogeneous and in perfect contact with the ATR crystal. For this reason, it has been extensively used to determine optical constants of liquids[38] as well as of selected polymeric surfaces[33]. It has been shown[21] that this methodology is also valid for anisotropic materials and that, for s-polarization, the transformed absorbance spectrum corresponds to the components of transition moments along the electric vector of the s-polarized light.

Beside the basic approaches, there are more advanced theories[39,40] that have utilized the multilayer surface model in an effort to deal with the situations where the conditions of other methodologies could not be met. For example, non-ideal contact between the crystal and the sample, limit sample thickness and the effect of the substrate on the ATR spectrum of a thin film could be taken into account. Several successful applications of these advanced approaches to polymer characterizations have been illustrated by Sellitti *et al.*[41]. In principle, the multilayer surface model can also be applied to the depth profiling of samples whose compositions are varied in the sample thickness direction[38].

In view of the existing considerations dealing with the analysis of ATR spectra, this study focuses on the effect of different methodologies on the I_a/I_b intensity ratio in polyethylene. Because of the complexity of the multilayer approaches, we only consider the differences between the intensity ratio measured from the raw ATR spectra and that from the absorbance spectrum obtained using the KKT and Fresnel reflectivity analysis.

Let us consider an ATR spectrum of polyethylene, as shown in *Figure 1A*. The spectrum was recorded at 45° incident angle with the sample machine direction perpendicular with the electric vector of the s-polarized light. *Figure 1B* illustrates the absorbance spectrum calculated from *Figure 1A* using the KKT and Fresnel's equation. It is apparent that the intensity ratio (I_a/I_b) of the 730 and 720 cm^{-1} bands in *Figure 1A* is much greater than that obtained from *Figure 1B*.

According to equation (3), by ratioing the ATR spectrum to the absorbance spectrum, one obtains the d_e dependence. Therefore, the difference between the ATR spectrum and the true absorbance spectrum can be rationalized by reconsidering the assumption used in deriving equations (4) and (5), the assumption of constant n_2, which is implied when the band ratioing technique is used on the raw ATR spectra. In this section, we will ignore this assumption and illustrate how the dispersion in n_2 can cause the difference between ATR and true absorbance spectra. *Figure 2B* is the real part of the refractive index of polyethylene, calculated from the ATR spectrum shown in *Figure 2A*. The d_e spectra obtained using equation (4) for various angles of incidence, but the same n_2 (*Figure 2B*), are shown in *Figure 3* and clearly illustrate that, for all angles of incidence, the d_e of the 730 cm^{-1} band is smaller than that at 720 cm^{-1}. The unequal d_e values of these two bands are responsible for the different intensity ratios of I_a/I_b measured from *Figures 1A* and *B*. The spectral distortion of *Figure 1A* relative to *B* is an example of perturbation between the two neighbouring absorption bands. A general discussion of this subject has been provided by Goplen *et al.*[35], who showed that the extent of perturbation increases with the maximum absorbance, the band overlap of the adjacent i.r. bands as well as the average refractive index of the sample.

With this in mind, let us examine how optical dispersions may affect distortion of strong ATR bands which, in turn, will influence the surface crystallinity measurements in polyethylene. For that reason, the amorphous phase content was calculated using raw ATR band intensities following procedures employed in reference 17 [equation (1)], and using ATR intensities modified by the KKT and Fresnel's equation. The 730 and 720 cm^{-1} bands were measured after Lorentzian curvefitting and the resulting calculated amorphous

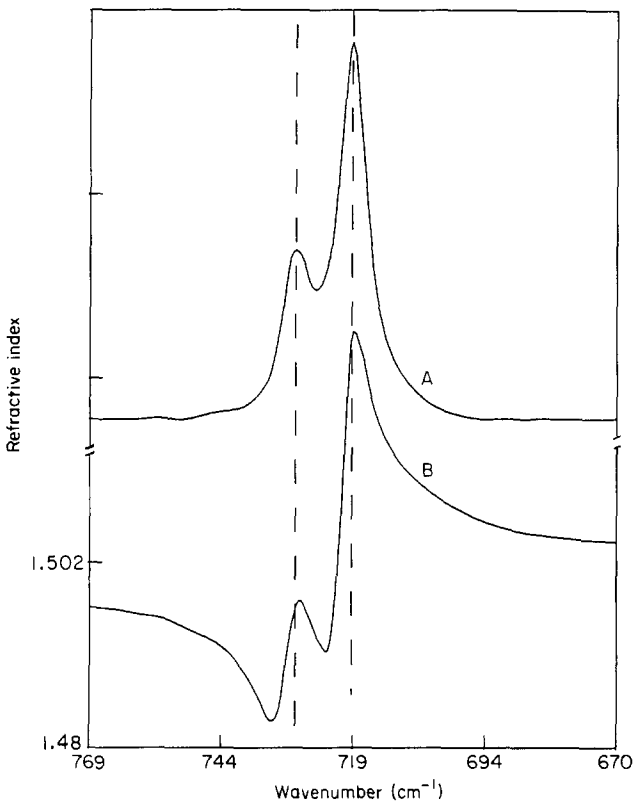

Figure 2 ATR *FT*i.r. spectrum (A) of polyethylene and the calculated real part of the refractive index spectrum (B)

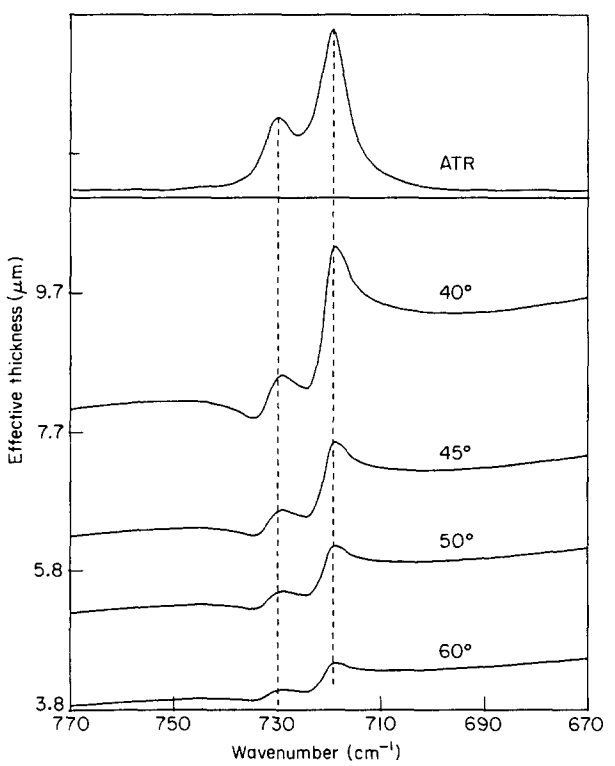

Figure 3 Effective thickness as a function of wavenumber for various angles of incidence calculated from *Figure 2B*

content was plotted as a function of the penetration depth. These results are shown in *Figure 4*. *Figures 4A* and *B* were obtained from the raw ATR spectra recorded with the sample machine direction aligned perpendicular and parallel to the electric vector of the s-polarized light, respectively. *Figures 4A'* and *B'* are the counterparts of *Figures 4A* and *B*, but were obtained after the KKT and Fresnel's relation analysis of the raw ATR spectra. As expected, significant intensity ratio differences between the raw ATR and the transformed absorbance spectra are reflected in differences in the amorphous contents calculated therefrom.

In view of the above considerations, it is quite obvious that the combination of the KKT and Fresnel's equation leads to substantially different results than those obtained by direct intensity measurements. Although the KKT approach also involves approximations when heterogeneous samples are considered, the direct intensity measurement from the raw ATR spectra contains assumptions, such as n_2 is a constant, which have been shown to have direct effects on the I_a/I_b intensity ratio. Therefore, the results from the KKT approach are more reliable than those obtained using raw ATR spectra. As a result, the former approach leads to the conclusion that the morphous content in polyethylene films is higher near the surface.

Analysis of the results presented in *Figure 4* also indicates that, depending upon the sample orientation with respect to the electric vector of the polarized i.r. light, there are substantial differences in the band intensities. Because the only difference between *Figures 4A* and *B* is the sample orientation during the ATR experiment, this difference is attributed to the molecular orientation. For that reason, the effect of molecular orientation on the intensity ratio of the 730 and 720 cm^{-1}

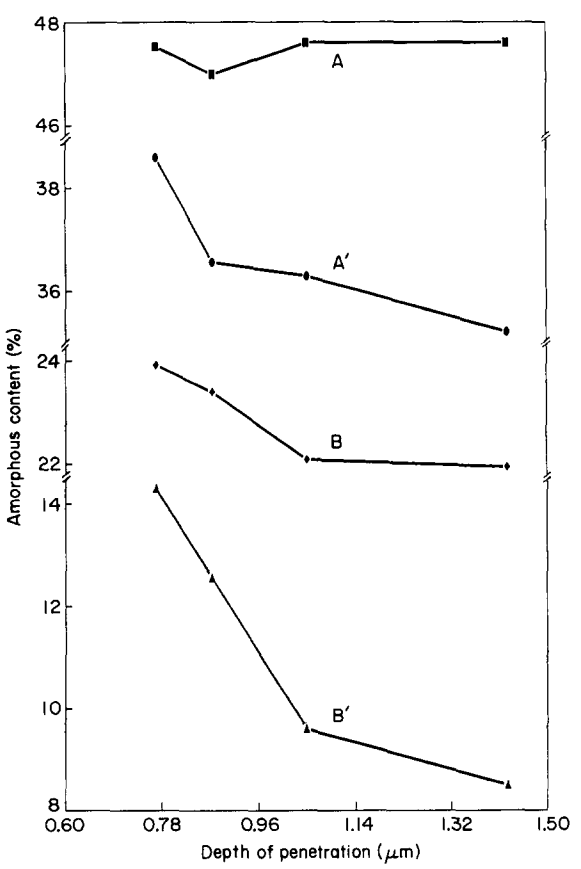

Figure 4 Amorphous content (%) as a function of the depth of penetration calculated from ATR spectra: (A) raw perpendicular polarization; (A') corrected perpendicular polarization; (B) raw parallel polarization; (B') corrected parallel polarization

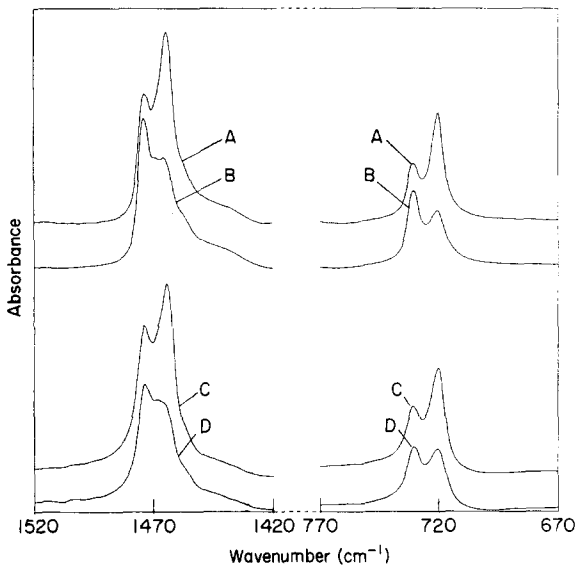

Figure 5 *FT*i.r. absorbance spectra of polyethylene film: (A) transmission perpendicular polarization; (B) transmission parallel polarization; (C) transformed ATR perpendicular polarization; (D) transformed ATR parallel polarization

bands and its effect on the surface crystallinity content will be addressed below.

It should be realized that, when using an ATR cell equipped with a rectangular internal reflectance element, the effect of preferred molecular orientation within the sample cannot be eliminated by using non-polarized light[21]. Even in transmission experiments, the incident light is inherently polarized due to instrument response, often referred to as the Crawford S-factor[42]. Therefore, it is first necessary to assess a preferred polyethylene surface chain orientation. *Figure 5* illustrates the CH_2 bending (1474 and 1464 cm^{-1}) and rocking (730 and 720 cm^{-1}) regions of a polyethylene spectrum. *Figure 5A* was recorded in a transmission mode of detection with the incident i.r. light polarized perpendicular to the machine direction of the sample, whereas in *Figure 5B* the light is in the parallel direction. *Figures 5C* and *D* are the same spectra recorded in the ATR mode at a 45° angle of incidence using the KRS-5 crystal and transformed using the KKT and Fresnel's reflectivity analysis. First, let us compare transmission spectra illustrated by *Figures 5A* and *B*. It appears that the intensity ratios of the 730 and 720 cm^{-1} bands are inverted when going from perpendicular (*Figure 5A*) to parallel (*Figure 5B*) orientations; namely $(I_a/I_b)_\perp < (I_a/I_b)_\parallel$. A similar trend is observed for ATR measurements (*Figures 5C* and *D*). The result shown in *Figure 5* is in good agreement with that previously reported in the literature[43].

Having established that the I_a/I_b ratio is sensitive to sample orientation, let us estimate the orientation of the crystalline phase near the surface and in the bulk of polyethylene. In order to establish the surface crystallinity content, a complete characterization of the surface molecular orientations is necessary[44] and such procedures require either ATR measurements using p-polarized light[45–47], transmission measurements with tilted angles[48] or polarization modulation studies for sensitivity enhancement[49]. In this study, the orientation of polyethylene crystallites will be measured using polarized transmission and ATR spectra of polyethylene, using the dichroic ratio method ($D = A_\parallel/A_\perp$, where $A_\parallel$ and $A_\perp$ are absorbances measured with the machine draw direction aligned parallel and perpendicular, respectively, to the electric vector of the polarized light).

Figure 6 illustrates the dichroic ratios of the 730 (*Figure 6A*) and 720 cm^{-1} (*Figure 6B*) bands in the corrected ATR spectra plotted as a function of the penetration depth at 720 cm^{-1}. For comparison, the dichroic ratios of the 730 (*Figure 6A'*) and 720 cm^{-1} (*Figure 6B'*) bands determined from the transmission spectra are also shown. To interpret the dichroic ratio results shown in *Figure 6*, its is necessary to realize the relationship between directions of the transition moment vectors of i.r. bands of interest and the axes of the crystalline unit cell. According to the literature[14], the direction of the transition moment vector for the 730 cm^{-1} band coincides with the *a* axis of an orthorhombic unit cell for polyethylene, whereas for the crystalline portion of the 720 cm^{-1} band the transition moment vector is aligned along the *b* axis[14]. Because the glass transition temperature of the amorphous polyethylene is much lower than the measurement temperatures, it is reasonable to assume that the orientations of molecular chains in the amorphous phase are random, and the non-unity dichroic ratio for the 720 cm^{-1} bands should be attributed to the crystalline contribution only.

First, let us consider the orientation of the *a* axis. *Figure 6A* shows that, within a given range of penetration depths, the dichroic ratio of the 730 cm^{-1} band changes slightly, but oscillates about unity. Because the transition moment vector for this band coincides with the *a* axis of an orthorhombic unit cell[14], the results presented in *Figure 6* indicate that the *a* axis of the unit cell is either randomly oriented within the film plane, or preferentially oriented perpendicular to the film plane direction. In contrast, *Figure 6A'* indicates that the dichroic ratio of this band measured from the transmission spectra is much greater reaching values of almost 1.4. This observation suggests that, in the core of the film, the *a* axis is predominantly oriented along the machine draw direction.

Similarly, *Figures 6B* and *B'* illustrate the dichroic ratio dependence for the band at 720 cm^{-1} obtained in ATR

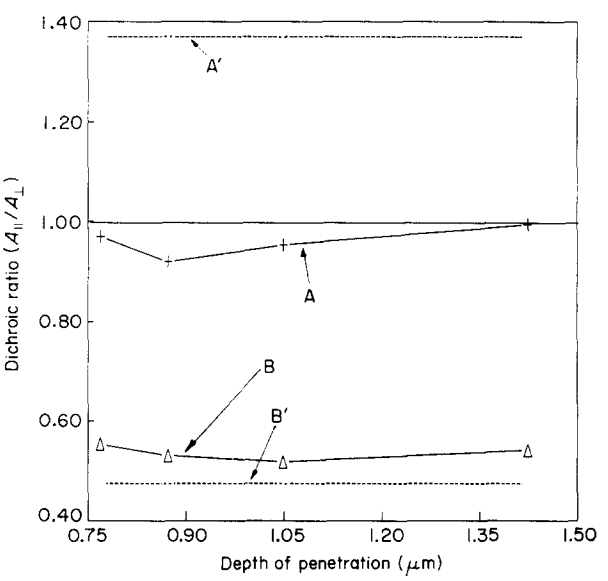

Figure 6 Dichroic ratio plotted as a function of depth of penetration: (A) 730 cm^{-1}, ATR; (B) 720 cm^{-1}, ATR; (A') 730 cm^{-1}, transmission; (B') 720 cm^{-1}, transmission

and transmission measurements, respectively. The fact that the dichroic ratios in all ATR and transmission spectra for the 720 cm^{-1} band are much smaller than unity indicates that the *b* axis of the unit cell is predominantly oriented perpendicular to the machine draw direction. It can also be seen from *Figure 6* that the dichroic ratio values for the 720 cm^{-1} band calculated from the ATR spectra are very close to that determined using transmission measurements. This observation indicates that there are no considerable changes in the *b* axis orientation when going from the surface into the bulk of the film.

It has been reported that for extruded polyethylene the *a* axis is parallel and the *b* axis is perpendicular to the extrusion direction[14]. When the polymer is stretched along that direction, the *a* axis changes its orientation to be perpendicular, whereas the *b* axis remains perpendicular to the direction of extrusion[14,50]. The results shown in *Figure 6* appear to be a combination of these two cases and are certainly a function of the polymer preparation. The differences in the orientation distribution, while going from surface to bulk, have been noted previously for polyethylene and other polymers[51,52] and this study further reinforces the fact that the orientation of crystalline components may significantly affect the I_a/I_b intensity ratio, and therefore the crystalline–amorphous content on a polyethylene surface.

CONCLUSIONS

These studies show that the crystallinity measurements in polyethylene at various surface depths are affected not only by ATR optics, but also by the crystalline phase orientation within the sample surface. This is demonstrated by the relative intensity changes of the CH_2 normal bending or rocking modes in the 1470 and 740 cm^{-1} regions, respectively. In order to use these bands for crystallinity measurements from ATR spectra, the ATR optical effects should be properly corrected.

ACKNOWLEDGEMENT

The authors are grateful to the National Research Electric Cooperative Association, Washington, DC, for partial support of this work.

REFERENCES

1 Bigg, D. M., Epstein, M. M., Fiorentino, R. J. and Smith, E. G. *J. Appl. Polym. Sci.* 1981, **26**, 395
2 Schneider, B., Jakes, J., Pivcova, H. and Doskocilova, D. *Polymer* 1979, **20**, 939
3 Rueda, D. R., Hidalgo, A. and Balta, F. J. *Spectrochim. Acta* 1978, **34**, 475
4 Glenz, W. and Peterlin, A. *J. Macromol. Sci. Phys.* 1970, **4**, 473
5 Zachmann, H. G. and Stuart, H. A. *Makromol. Chem.* 1961, **44/46**, 622
6 Stein, R. S. and Norris, F. H. *J. Polym. Sci.* 1956, **21**, 381
7 Baker, C. and Maddams, W. F. *Makromol. Chem.* 1976, **177**, 437
8 Snyder, R. G. and Poore, M. W. *Macromolecules* 1973, **6**, 708
9 Zerbi, G. *Pure Appl. Chem.* 1971, **236**, 499
10 Opaskar, C. G. and Krimm, S. *Spectrochim. Acta* 1965, **21**, 1165
11 Willbourn, A. H. *J. Polym. Sci.* 1959, **34**, 569
12 Matsuda, H., Okada, K., Takese, T. and Yamamoto, T. *J. Chem. Phys.* 1964, **41**, 1527
13 Nikitin, V. N. and Pokrovskii, E. I. *Doklady Akad. Nauk SSSR* 1954, **95**, 109
14 Tobin, M. C. and Carrano, M. J. *J. Polym. Sci.* 1957, **24**, 93
15 Wedgewood, A. R. and Seferis, J. C. *Pure Appl. Chem.* 1983, **55**, 873
16 Okada, T. and Mandelkern, L. *J. Polym. Sci., Polym. Phys. Edn* 1967, **5**, 239
17 Zerbi, G., Gallino, G., Fanti, N. D. and Baini, L. *Polymer* 1989, **30**, 2324
18 Dothee, D., Vigourreux, J. M. and Camelot, M. *Polym. Degrad. Stab.* 1988, **22**, 161
19 Abbate, S., Gussoni, M. and Zerbi, G. *J. Chem. Phys.* 1979, **70**, 3577
20 Harrick, N. J. 'Internal Reflection Spectroscopy', Interscience Publishers, New York, 1967
21 Bardwell, J. A. and Dignam, M. *Spectrochim. Acta 1988*, **44A**, 1435
22 Ohta, K. and Ishida, H. *Appl. Spectrosc.* 1988, **42**, 952
23 Bertie, J. E. and Eysel, H. H. *Appl. Spectrosc.* 1985, **39**, 392
24 Huong, J. B. and Urban, M. W. *Appl. Spectrosc.* in press
25 Harrick, N. J. 'Internal Reflection Spectroscopy', Interscience Publishers, New York, 1967, p. 30
26 Born, M. and Wolf, E. 'Principles of Optics', 5th Edn, Pergamon Press, Oxford, 1975
27 Harrick, N. J. 'Internal Reflection Spectroscopy', Interscience Publishers, New York, 1967, p. 43
28 Mirabella, J. F. M. *Spectroscopy* 1990, **5**, 21
29 Koenig, J. L., D, Esposito, L. and Antoon, M. K. *Appl. Spectrosc.* 1977, **31**, 292
30 Mirabella, J. F. M. *J. Polym. Sci., Polym. Phys. Edn* 1985, **30**, 861
31 Mirabella, J. F. M. *Appl. Spectrosc. Rev.* 1985, **21**, 45
32 Crawford Jr, B., Goplen, T. G. and Swanson, D. in 'Advances in Infrared and Raman Spectroscopy' (Eds R. J. H. Clark and R. E. Hester), Vol. 4, Heyden, London, 1980, Ch. 2, p. 47
33 Graf, R. T., Koenig, J. L. and Ishida, J. in 'Fourier Transmission Infrared Characterization of Polymers' (Ed. H. Ishida), Plenum Press, New York, 1987, p. 385
34 Graf, R. T., Koenig, J. L. and Ishida, J. in 'Fourier Transmission Infrared Characterization of Polymers' (Ed. H. Ishida), Plenum Press, New York, 1987, p. 1
35 Goplen, T. G., Cameron, D. G. and Jones, R. N. *Appl. Spectrosc.* 1980, **34**, 652
36 Hawranek, J. P. and Jones, R. N. *Spectrochim. Acta* 1976, **32A**, 99
37 Graf, R. T., Koenig, J. L. and Ishida, H. *Appl. Spectrosc.* 1985, **39**, 405
38 Goplen, T. G., Cameron, D. G. and Jones, R. N. *Appl. Spectrosc.* 1980, **34**, 657
39 Heavens, O. S. 'Thin Film Physics', Methuen & Co. Ltd, London, 1970, Ch. 6
40 Stuchebryukov, S. D., Vavkushevsky, A. A. and Rudoy, V. M. *Surface Interface Anal.* 1984, **6**, 29
41 Sellitti, C., Koenig, J. L. and Ishida, H. *Mater. Sci. Eng.* 1990, **A126**, 235
42 Crawford Jr, B., Goplen, T. G. and Swanson, D. in 'Advances in Infrared and Raman Spectroscopy' (Eds R. J. H. Clark and R. E. Hester), Vol. 4, Heyden, London, 1978, p. 47
43 Hsu, S. L. in 'Comprehensive Polymer Science, Vol. 1, Polymer Characterization' (Eds C. Booth and C. Price), 1st Edn, Pergamon, Oxford, 1989, p. 429
44 Sung, C. S. P. *Macromolecules* 1983, **16**, 193
45 Flournoy, P. A. and Schoeffers, W. J. *Spectrochim. Acta* 1966, **22**, 5
46 Hansen, W. H. *Spectrochim. Acta* 1965, **21**, 815
47 Hobbs, J. P., Sung, C. S. P., Krishnam, K. and Hill, S. *Macromolecules* 1983, **16**, 193
48 Fina, L. J. and Koenig, J. L. *J. Polym. Sci., Polym. Phys. Edn* 1986, **24**, 2509
49 Stein, R. S. *J. Appl. Polym. Sci.* 1961, **5**, 96
50 Read, B. E. and Stein, R. S. *Macromolecules* 1968, **1**, 116
51 Sung, C. S. P. *Macromolecules* 1981, **14**, 591
52 Tshmel, A. E., Vettegren, V. I., Zolotarev, V. M. and Ioffe, A. F. *Macromol. Sci. Phys.* 1982, **B21**, 243